Journal of Environmental Management 314 (2022) 115064

Contents lists available at ScienceDirect

Journal of Environmental Management

journal homepage: www.elsevier.com/locate/jenvman

Research article

Distribution of radiocesium and its controlling factors under the Japanese cedar canopies

Hiroaki Kato *, Yuichi Onda, Keita Maejima

Center for Research in Isotopes and Environmental Dynamics, University of Tsukuba, Ibaraki, 305-0006, Japan

ARTICLE INFO

Keywords:
Fukushima Daiichi Nuclear Power Plant accident
Forest floor
Cedar stand
^{137}Cs
Spatial variability

ABSTRACT

This study investigated the spatial distribution of radiocesium deposited by the Fukushima Daiichi Nuclear Power Plant accident in a densely planted Japanese cedar stand. Systematic grid sampling was conducted to determine ^{137}Cs inventories in the layers of deposited organic material and mineral soil at two different spatial scales (hillslope [60 m^2] and small [1 m^2]). The results showed that ^{137}Cs inventories along the hillslope were heterogeneously distributed, with coefficients of variation for the deposited organic material and mineral soil layers of 46.4% and 48.9%, respectively. The ^{137}Cs inventory in each layer tended to show a lognormal distribution. The correlation between the ^{137}Cs inventories in deposited organic material and mineral soil in the same sampling grid was weak. The controlling mechanisms of the ^{137}Cs inventories in the litter and mineral soil layers differed due to differences in the underlying key processes, such as canopy-forest floor transfer due to hydrological and biological processes. No significant correlation was found between the distance from the nearest tree trunk and the ^{137}Cs inventory in the deposited organic layer at each sampling point. In contrast, the ^{137}Cs inventory in the soil tended to increase as the distance from the nearest tree trunk increased at both the hillslope and small scales. It was found that the initial spatial patterns of ^{137}Cs in the soil layer due to atmospheric deposition were preserved in the cedar stand. Finally, we tested the effects of soil sampling density on the reliability of mean soil ^{137}Cs inventory estimations in the cedar stand. The results indicated that a soil sampling area greater than 0.06 m^2 at the hillslope scale and 0.008 m^2 at the small scale enabled the mean ^{137}Cs inventory to be estimated with an uncertainty of less than 20% in the cedar stand.

Credit author statement

Hiroaki KATO: Conceptualization, Methodology, Validation, Formal analysis, Investigation, Data curation, Writing original draft, Visualization, Funding acquisition. Yuichi ONDA: Conceptualization, Validation, Resources, Writing, Project administration, Funding acquisition. Keita MAEJIMA: Methodology, Validation, Formal analysis, Investigation,

1. Introduction

Radiocesium released into the atmosphere due to the Fukushima Daiichi Nuclear Power Plant accident has caused extensive radioactive contamination of forests over a wide area, mainly in eastern Japan (Butler, 2011). It is estimated that about 70% of the radiocesium deposited in Japan has accumulated in forest areas (Hashimoto et al., 2012; Kato and Onda, 2018; Kato et al., 2019a). Understanding the distribution and migration of radioactivity in Japanese forests is therefore essential to assess the ongoing environmental impact of the accident. However, forest ecosystems are characterized by a large spatial variability of radiocesium due to the complexities of water and material cycling (Takada et al., 2016; Kato et al., 2017, 2018a, 2019b; Hisadome et al., 2020); therefore, an extensive effort is required to characterize the overall status of radioactive contamination in forests.

When radiocesium is deposited from the atmosphere into a forest, most of it is initially intercepted by the canopy (Ronneau et al., 1987; Bunzl et al., 1989; Schimmack et al., 1993; Kliashtorin et al., 1994; Melin et al., 1994; Sombré et al., 1994; Itoh et al., 2015; Kato et al., 2012, 2017, 2019b). Much of the radiocesium is immediately leached from branches and leaves by rainwater, washed out of the canopy, and transferred to the forest soil (Kato et al., 2012, 2017, 2019b; Kato and Onda, 2014; Loffredo et al., 2014, 2015; Endo et al., 2015; Nishikiori et al., 2015; Niizato et al., 2016). The amount of dissolved radiocesium

* Corresponding author. Center for Research in Isotopes and Environmental Dynamics, University of Tsukuba Laboratory of Advanced Research A503, 1-1-1 Tennodai, Tsukuba, Ibaraki, 305-0006, Japan.
E-mail address: kato.hiroaki.ka@u.tsukuba.ac.jp (H. Kato).

https://doi.org/10.1016/j.jenvman.2022.115064
Received 22 December 2021; Received in revised form 7 April 2022; Accepted 9 April 2022
Available online 18 April 2022

transferred from the canopy to the forest floor decreases exponentially with time, with the primary transfer pathway of canopy radiocesium gradually switching to biological pathways, such as litterfall (Teramage et al., 2014a; Endo et al., 2015; Niizato et al., 2016; Kato et al., 2017, 2019b; Hisadome et al., 2020). The accumulation of ^{137}Cs on the forest floor is a result of the combination of the initial interception by the forest canopy and the subsequent inputs from water and litterfall.

The canopy structure governs the depositional flux of ^{137}Cs from the canopy to the forest floor (Loffredo et al., 2014, 2015; Hisadome et al., 2020). Because the canopy structure varies greatly from tree to tree, ^{137}Cs on the forest floor can be heterogeneously distributed on the forest floor. Loffredo et al. (2015) reported that the amount of canopy ^{137}Cs leached by throughfall is dependent on the canopy density; thus, forest floor locations under dense canopy cover tend to accumulate more ^{137}Cs. On the other hand, Hisadome et al. (2020) found that the more significant the litterfall, the greater the ^{137}Cs flux to the forest floor. These studies suggest that the ^{137}Cs flux to the forest floor due to water and litterfall are strongly dependent on canopy structure. However, the actual spatial distribution of ^{137}Cs under forest canopies and how canopy structure affects the accumulation of ^{137}Cs on the forest floor is poorly understood.

Kato et al. (2018a) investigated the spatial distribution of ^{137}Cs on the forest floor of coniferous (cedar) and mixed forest stands during the first year after the initial fallout following the Fukushima accident. Repeated in-situ measurements of ^{137}Cs using a portable Ge gamma-ray detector indicated that ^{137}Cs radioactivity on the forest floor tended to be higher in the gap area than under the canopy. Takada et al. (2016) reported that canopy cover density affects the spatial pattern and the coefficient of variation (CV) of the atmospherically deposited ^{137}Cs on the forest floor. These studies have indicated that during the early phase of the initial atmospheric deposition, the variation of canopy coverage affects the initial canopy interception of the atmospherically deposited ^{137}Cs, and thus the spatial pattern of ^{137}Cs on the forest floor. However, there is no available monitoring data indicating how the distribution of ^{137}Cs on the forest floor will change in the long term.

The Fukushima forests have been decontaminated to reduce radiation exposure. This has been achieved by removing the litter layer of the forest floor up to 20 m from the forest edge where it borders residential areas (Forestry Agency, 2014). Most of the ^{137}Cs reached the forest floor before the major decontamination campaign, and therefore this decontamination method was considered practical to reduce the ambient dose rate. However, the effect of decontamination can be limited due to the continuous ^{137}Cs deposition by litterfall over the long term. Therefore, investigating the spatial distribution of radiocesium in a contaminated forest will clarify the role of litterfall on the ^{137}Cs depositional flux and its spatial heterogeneity on the forest floor.

The ambient dose rate on the forest floor changes over time due to the changing spatial distribution of radiocesium in the forest (Gonze et al., 2015, 2016; Malins et al., 2016; Kato et al., 2018b). The radiocesium inventory in the uppermost surface soil and litter layer is the primary contributor to the ambient dose rate on the forest floor (Imamura et al., 2018). Previous studies have reported that the ambient dose rate on the forest floor persists over time. Therefore, no significant redistribution of radiocesium occurs due to the lateral transport of sediment and deposited organic material along hillslopes (Koarashi et al., 2014; Atarashi-Andoh et al., 2015; Imamura et al., 2018). Nevertheless, on a steep forest hillslope, the lateral transport of sediment and deposited organic material can initiate the transfer of radiocesium along the hillslope (Fukuyama et al., 2008). Therefore, long-term monitoring of the radiocesium distribution on the forest floor is essential to determine the temporal evolution of the ambient dose rate and radiocesium cycling in forest ecosystems.

Soil sampling has been conducted to investigate the spatial patterns of radiocesium in forests, with the results showing that radiocesium is heterogeneously distributed over forest floors (Khomutinin et al., 2004, 2020; Takada et al., 2016; Kato et al., 2018a; IAEA, 2019). An optimized sampling strategy is required to obtain a representative radiocesium inventory for a target forest floor by determining the spatial distribution patterns of radiocesium based on geostatistical approaches (Khomutinin et al., 2004, 2020; IAEA, 2019). Khomutinin et al. (2020) applied a geostatistical analysis to derive the minimum sample number required to obtain a representative radiocesium inventory for various land uses and fallout types in the areas affected by fallout from the Chernobyl reactor accident. They proposed a simple method for assessing the minimum sample size required to estimate the median or geometric mean of radionuclide soil contamination within a certain uncertainty for single or composite samples. However, no sampling guidelines are available for Fukushima-derived radiocesium in Japanese forest environments.

In this study, the spatial distribution of radiocesium deposited following the Fukushima Daiichi Nuclear Power Plant accident was investigated in a young, densely planted Japanese cedar forest, for which Kato et al. (2018a) reported a high canopy interception rate. Systematic grid sampling was conducted to determine the ^{137}Cs inventories in the layers of deposited organic material and mineral soil at two different spatial sampling scales (hillslope [60 m^2] and small [1 m^2]). The factors determining the ^{137}Cs inventory on the forest floor were determined using monitoring data. Specifically, the effects of hydrological and biological transport pathways on radiocesium accumulation on the forest floor were examined. We also investigated whether canopy cover and distance from trees can explain the ^{137}Cs inventory on the forest floor. Finally, sampling guidelines for estimating the representative ^{137}Cs inventory in mineral soil layers were developed based on a geostatistical analysis of the measured heterogeneity of ^{137}Cs on the forest floor.

2. Materials and methods

2.1. Study site description

The study site was located in Kawamata Town of Fukushima Prefecture, 40 km northwest of the power plant (Figure S-1). The total ^{137}Cs fallout following the Fukushima accident was 442 kBq/m^2. Radiocesium deposition from other primary depositional sources, such as global fallout in Japan, has been reported to be around 3–4 kBq/m^2 (Sakaguchi et al., 2010; Teramage et al., 2014b). The pre-Fukushima accident-derived fallout flux is <1% of the total ^{137}Cs inventory at the study site. Therefore, the ^{137}Cs data in this study can be regarded as almost exclusively derived from the Fukushima accident. A young cedar stand was selected as the experimental forest site (Table 1, Figure S-2). The stand was 22 years old at the time of the soil and litter sampling experiment. The experimental forest site was decontaminated in October 2013 (Figure S-3). Organic materials on the forest floor were removed by hand to minimize the disturbance of surface soil. Litter and soil sampling were conducted in the experimental forest on August 24–25, 2015.

The change of the ^{137}Cs inventory in the litter and soil layers in the experimental plot was estimated based on previous studies in the same

Table 1
Stand characteristics of the experimental forest. Biomass and LAI data were derived from the estimation results of Coppin et al. (2016).

Stand property	Young cedar
Stand age (y)	22
Stem density (stem/ha)	2,400
Tree height (m)	<15
Slope (degree)	33
Needle biomass (kg/m^2)	3.31 (live) 0.71 (dead)
LAI (m^2/m^2)	10.3
^{137}Cs fallout (kBq/m^2)	442

forest stand targeting the transfer of ^{137}Cs from the canopy to forest floor via hydrological and biological pathways (Loffredo et al., 2014, 2015; Kato et al., 2017, 2019b; Hisadome et al., 2020) and the downward migration of ^{137}Cs in the deposited organic layer and underlying soil profile (Takahashi et al., 2015, 2018). The ^{137}Cs removed by the decontamination was estimated to account for 20% of the total ^{137}Cs inventory on the forest floor (413 kBq/m^2 at the time the study site was decontaminated). The additional input of ^{137}Cs during the period between decontamination and soil sampling was 9 kBq/m^2 in total (2% of the initial deposition), of which 5 kBq/m^2 was received through hydrological pathways (e.g., throughfall and stemflow) and 4 kBq/m^2 occurred due to litterfall. The organic materials deposited on the forest floor consisted of only the newly deposited litterfall on the ground surface during the period between the time of decontamination and soil sampling (26 months).

2.2. Sampling of the organic layer and underlying soil

2.2.1. Hillslope scale plot

An experimental plot approximately 6.9 m long and 8.5 m wide (covering 47.6 m^2) was selected on the forested hillslope. The whole area was located on a north-facing slope (slope 33°). No substantial surface runoff occurred on this slope during normal rainfall events, with all the rainfall that reached the forest floor infiltrating into the soil layer. There was very little understory vegetation on the forest floor due to the closed-canopy coverage and low light conditions. The experimental plot was divided into 49 grids to investigate the spatial distribution of ^{137}Cs on the forest floor in this study area (Fig. 1, Figure S-4a). The 49 grids were centered on a fixed point for continuous in-situ measurements using a portable germanium γ-ray detector (Kato et al., 2018a). In-situ measurements for determining the radiation dose due to ^{137}Cs on a forest floor immediately after the accident were reported by Kato et al. (2018a). However, the ^{137}Cs inventories in the litter and soil layers were not evaluated due to the indirect survey method.

2.2.2. Small scale plots

The small scale plots were selected within the hillslope scale plots, with grids 3–5 selected as a detailed sampling area (Fig. 1, Figure S-4b). The grid area was divided into 100 sub-grids. The survey in this grid area was referred to as “100-point sampling".

2.2.3. Sampling design

Sampling of the litter and soil layers was conducted as follows. The survey was conducted on August 24, 2015. First, all the litter material within the grids was collected from the hillslope scale plot (Figure S-5a, b). The litter material lying across the boundary of grids was cut at the boundary using scissors. The collected litter was separated into branches and leaves, and then weighed (Figure S-5c,d). The total collected sample mass was reduced by the quadrant method before being sealed in a polyethylene bag for laboratory analysis. Soil layers were sampled using a 100 ml stainless steel cylinder (DIK-1801) with a diameter of 50 mm and height of 50 mm. Sampling was performed at two depths, 0–5 and 5–10 cm, at five locations in the center, upper, and lower corners within the target grid area of the hillslope-scale plot (Figure S-5e). The five soil core samples were mixed at the field site and then sealed in a polyethylene bag. The representative concentration and inventory values of ^{137}Cs in the target grid were determined.

For the small scale plot, soil (0–5 and 5–10 cm layers) was collected in each sub-grid (Figure S-4b). Two stainless steel cylinder core samplers were connected to collect soil to a depth of 10 cm. After inserting the core sampler to the target depth (10 cm) in each grid of the small-scale plot, the sampler was separated at the joint to obtain the samples from the 0–5 and 5–10 cm layers, respectively.

The collected samples were oven-dried at 105 °C for 24 h and then weighed to obtain the total dry weight. Litter samples were crushed using a mixer, whereas soil samples were homogenized using a dust-free

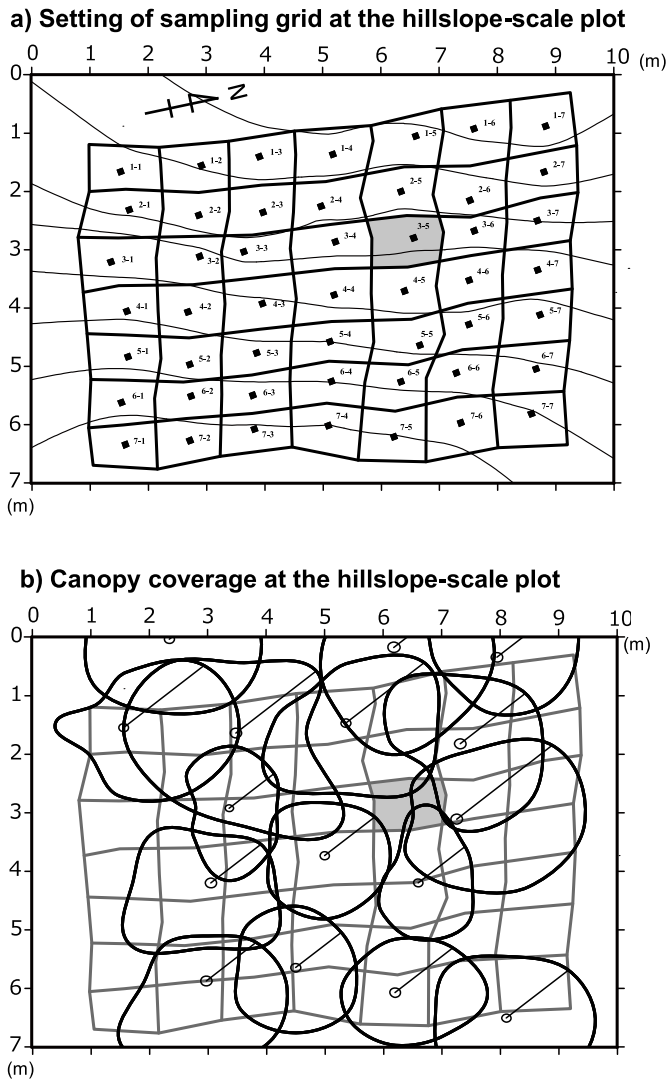

Fig. 1. Setting of the sampling grids and the canopy projection area in the hillslope experimental plot. The forty-nine grids are located within the experimental plot. The black symbols in the upper figure a) show the fixed 49 measurement points for the repeated in-situ measurement of radioactivity in Kato et al. (2018a). The grid area of grey color in the lower figure b) denotes the location of the small-scale plot.

automatic crushing sieve (DIK-2610). The samples were sealed in 100-mL capacity polystyrene U-shaped containers (U-8 container), and the ^{137}Cs radioactivity was measured using a germanium γ-ray detector. Gamma-ray emissions at energies of 662 keV (^{137}Cs) were measured using a high-purity n-type germanium coaxial gamma-ray detector (EGC25-195-R; Canberra-Eurisys, Meriden, CT, USA) coupled to an amplifier (PSC822; Canberra-Eurisys) and multichannel analyzer (DSA1000; Canberra, Lingolsheim, France). The measurement system was calibrated using standard gamma sources with different materials and sample heights. All radioactivity measurements were corrected for radioactive decay between the time of sample collection and radiation detection. The standard deviations in the text and table represent the error in counting statistics.

3. Results and discussion

3.1. Measured spatial patterns of radiocesium on the forest floor

The spatial patterns of ^{137}Cs on the forest floor determined by the field sampling of deposited organic material and soil are shown in Figs. 2

and 3. The ^{137}Cs inventories at the 49 locations at the hillslope scale and 100 locations at the small scale were used to identify the spatial distribution of ^{137}Cs on the forest floor.

There were no obvious similarities in the spatial patterns of the ^{137}Cs inventory in the litter and soil layers at the hillslope scale. The ^{137}Cs inventory in the litter layer was larger in the area of overlapped canopy coverage (Fig. 2, grids 2–5 and 6–2). In contrast, the ^{137}Cs inventory in the soil layer was more significant in the peripheral areas of the cedar canopies (Fig. 2, grid 4–7). The ^{137}Cs inventories in the uppermost surface layer (0–5 cm layer) and the underlying sub-layer (5–10 cm layer) had similar spatial patterns at the hillslope scale (Fig. 2). On the other hand, the ^{137}Cs inventories in the uppermost surface layer were poorly correlated with the underlying sub-layer in the small scale plots (Fig. 3).

The ^{137}Cs inventories in the 49 measurement grids in the hillslope scale experiment ranged from 150 to 920 kBq/m^2 (n = 49, mean: 390 kBq/m^2, standard deviation (SD): 170 kBq/m^2), whereas the range for the 100 measurement grids in the small scale experiment was 124–1072 kBq/m^2 (n = 100, mean: 584 kBq/m^2, SD: 204 kBq/m^2). The CV value for the total ^{137}Cs inventory in soils at the hillslope scale was 43.4%. In contrast, the total inventory for both the deposited organic material and soil within the small scale plot was 35.0%. These results showed that the ^{137}Cs inventories along the forest hillslope were heterogeneously distributed.

Histograms of the measured ^{137}Cs inventory at the hillslope and small scales are presented in Fig. 4. The ^{137}Cs inventory in each layer followed a lognormal distribution. At the hillslope scale, the coefficients of variation for the ^{137}Cs inventory in the 0–5 and 5–10 cm deep soil layers were 44.7% and 90.7%, respectively. At the small scale, the coefficients of variation for the ^{137}Cs inventory in the 0–5 and 5–10 cm deep soil layers were 33.0% and 110%, respectively. In both the hillslope and small scale plots, the coefficients of variation for the layers of deposited organic material and the uppermost surface soil (0–5 cm layer) were in a similar range, but the CV obtained in the 5–10 cm layer was more significant than in the 0–5 cm layer.

Khomutinin et al. (2004, 2020) reported that ^{137}Cs was present in a spatially lognormal distribution under various land uses, including forest areas. The ^{137}Cs inventory distribution obtained for the deposited organic material, and the 0–5 and 5–10 cm soil layers had a lognormal distribution ($p < 0.05$). The significance of $p < 0.05$ was determined based on the Kolmogorov-Smirnov test.

An average ^{137}Cs contamination of 58.7 kBq was present in the litter layer (the total needle and branch contamination represented 15.1% of the total aerial inventory) (Fig. 5). Cesium-137 is mostly present in the litter layer on a forest floor immediately after deposition, and with time it migrates downward into the soil layer (Fujii et al., 2014; Takahashi et al., 2015, 2018). At the study site, the litter layer was removed once during a decontamination procedure in October 2013; therefore, the litter layer sampled in this study migrated from the tree canopy during the period from October 2013 to August 2015. The measured amount of ^{137}Cs was therefore transferred from the tree canopy to the forest floor 2–4 years after deposition.

Cesium-137 in the soil is limited to the uppermost soil layer (Takahashi et al., 2015, 2018; Imamura et al., 2020), and its vertical distribution decreases exponentially with depth (Teramage et al., 2014b; Takahashi et al., 2015, 2018; Imamura et al., 2020). It was found that 68.7% of the total ^{137}Cs on the forest floor was present in the 0–5 cm soil layer (Fig. 5). Kato et al. (2017) reported that the transfer of ^{137}Cs from the tree canopy to the forest floor decreases with time after deposition. Therefore, most of the ^{137}Cs in the litter layer was likely to have been transferred to the underlying soil layer before the forest decontamination.

The relationship between the weight of litter and the ^{137}Cs inventory is shown in Fig. 6. A correlation was found between the two parameters, suggesting that the inventory value of fallen leaves and branches was weight-dependent. A close correlation between the deposition flux of litter mass and ^{137}Cs was reported in a previous study (Hisadome et al., 2020). The variation of the ^{137}Cs concentration in fallen litter material

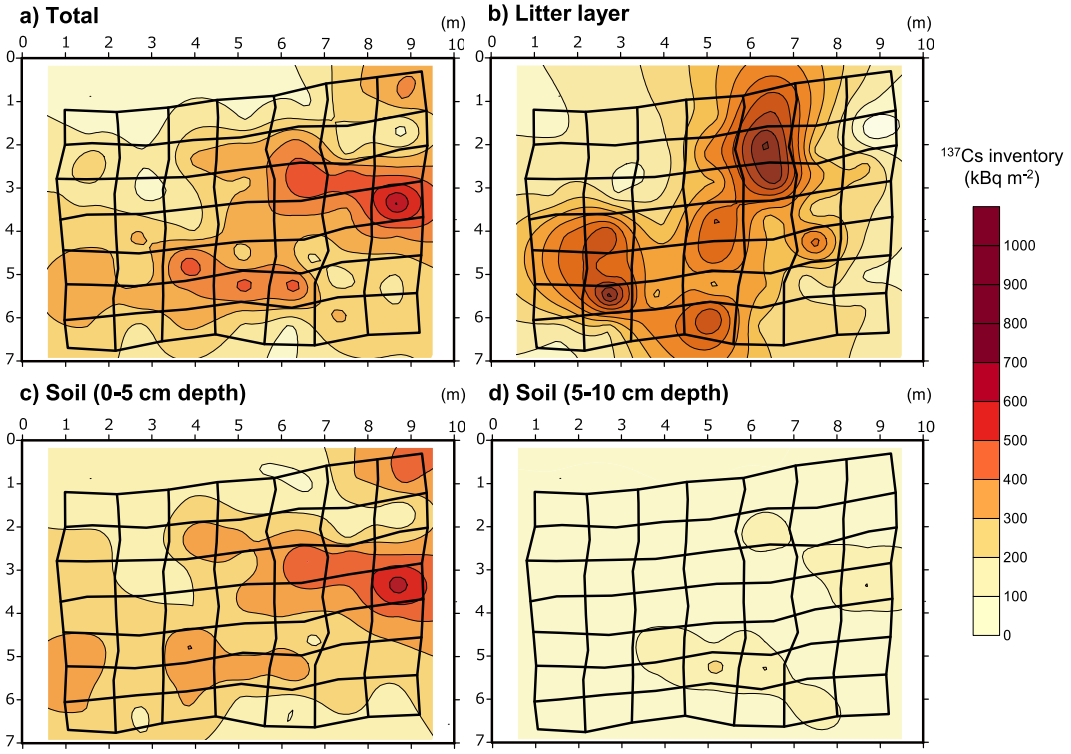

Fig. 2. The spatial patterns of ^{137}Cs inventory at hillslope scale within the experimental plot. The inventory of the litter layer is the actual measured value multiplied by 10 to match the scale of the legend.

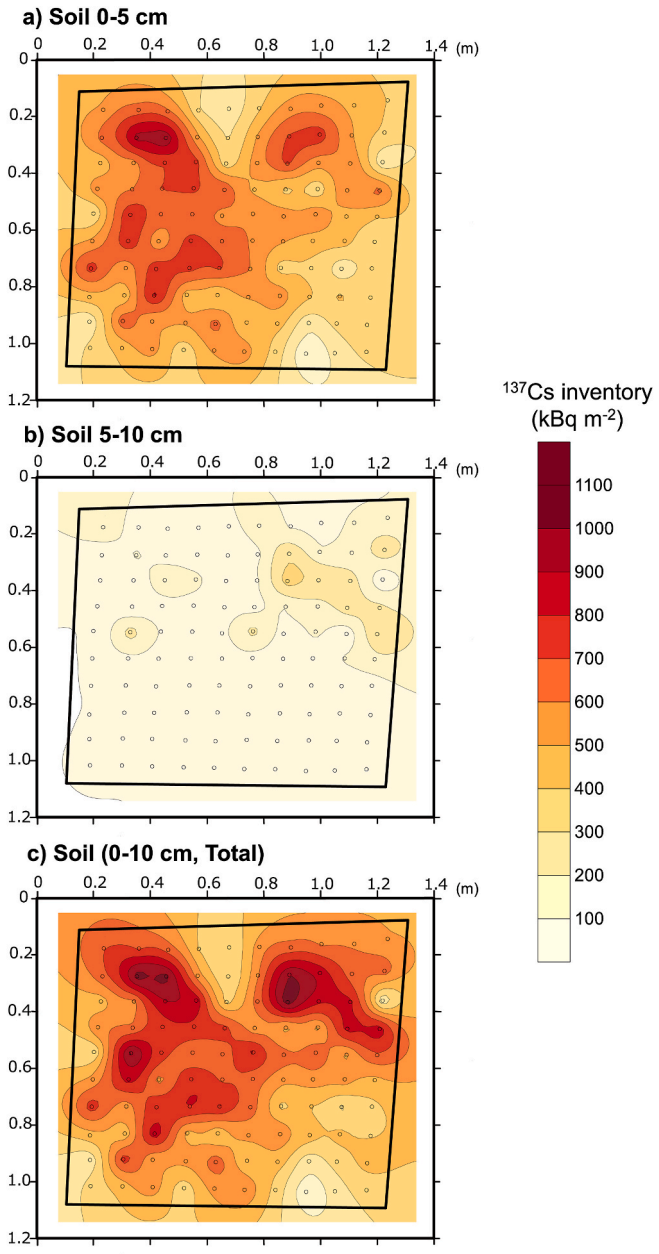

Fig. 3. Spatial patterns of ^{137}Cs inventory at small scale within the experimental plot. The rectangle line in the map shows the boundary of the small-scale plot.

was small; therefore, the litter depositional flux was a determinant of the ^{137}Cs input to the forest floor in the studied forest stand.

The relationship between the ^{137}Cs inventory in the 0–5 and 5–10 cm soil layers in each grid at the hillslope and small scales is shown in Fig. 7. A weak correlation was found at the hillslope scale between the uppermost (0–5 cm) and underlying (5–10 cm) soil layers. On the other hand, there was no clear correlation found in the small-scale plots. These results suggest that the spatial pattern of the ^{137}Cs inventory in the uppermost and the underlying soil layers could be roughly defined by the depositional flux of ^{137}Cs from the canopy to forest floor at the hillslope scale; however, the effects of vertical penetration from the surface to deeper horizon were less pronounced at the small scale.

The distribution of heavy metals among different soil horizons generally shows slight vertical variation. However, vertical discontinuities of heavy metals can be observed when the composition of pedological material differs among soil horizons (Palumbo et al., 2000; Martínez Cortizas et al., 2003; Conde Bueno et al., 2008). Nevertheless, the forest soils in this study (0–5 and 5–10 cm) both consist of the same A horizon of Andisol, which is characterized by low bulk density (0.33 g/cm^3) and a high macropore content (26.4%) (Takahashi et al., 2018). To understand the distribution characteristics of radiocesium in the studied soils, it is necessary to consider the factors that cause the heterogeneity unique to forest soils from two viewpoints: the adsorption mechanism to the solid phase of soil and the non-uniform influx into the soil profile.

Regarding the former, the adsorption of radiocesium on the solid phase of soil is affected by the composition and content of clay minerals (Cremers et al., 1988; Koarashi et al., 2012; Fujii et al., 2014). The type and abundance of clay minerals determine the retention capacity of radiocesium by absorption and fixation to alternative layers of clay minerals. Their horizontal and vertical distribution characteristics can influence the distribution of radiocesium in the soil profile. In addition, the presence of abundant organic matter and humic substances in forest soils enhances or reduces radiocesium adsorption to the solid phase of soil (Dumat and Staunton, 1999; Fan et al., 2014; Tatsuno et al., 2020). In addition, the exudates from roots and products of rhizosphere microorganisms control the adsorption of radiocesium to the solid phase of soil (Wendling et al., 2005; Chiang et al., 2011). Thus, heterogeneity in soil physicochemical and biogeochemical interactions between plants and soil could affect the distribution of radiocesium retention in the soil layer. No studies have yet discussed the relationship between the heterogeneity of radiocesium within the soil layers of the same forest area.

Regarding the latter viewpoint, uneven rainwater infiltration in forest soils can affect the amount of dissolved matter in the soil layer and lead to the maldistribution of pathways. In surface layers, channels formed by root distribution and soil animal activity are major regulators of water and solute movement in forest soils, and consequently affect the distribution of materials in the soil layer (Bengough, 2012; Tracy et al., 2013; 2013; Zhang et al., 2015). Particularly in conifer forest stands, greater vertical and horizontal spatial variability in preferential flow paths has been reported, transporting water and solutes to deeper soils (Luo et al., 2019). Furthermore, stemflow percolates into the tree base and then generates a bypass flow along the roots, which allows water to flow vertically and laterally (Liang et al., 2009, 2011). Thus, in forest soil layers with well-developed root systems, solutes are transported through the soil layer via complex rainwater infiltration pathways, but few studies have linked this to radiocesium distribution.

The transport pathways of radiocesium in forest soil layers are complex, indicating that soil physics, rainwater infiltration, and the resulting heterogeneity of solute transport control its distribution in soil layers. Our findings suggest that the factors that govern the transport pathways of ^{137}Cs in soil layers differ depending on the scale. At the slope scale, the average sample size was ~1 m^2—which masked the effects of complex rainwater infiltration processes at the micro-scale and the heterogeneity of soil physical properties and clay mineral distribution—and the surface and subsoil inventories were likely correlated. On the other hand, since the distribution was studied at a micro-scale (0.1-m grid), it is possible that there was no correlation between surface and subsoil ^{137}Cs inventories due to deep infiltration by preferential flow and non-vertical transport by bypass flow within the root system. This indicates the possibility of using accident-derived radiocesium remaining in the soil as a tracer to evaluate the infiltration mechanism of substances dissolved into the soil layer in forest soils.

3.2. Influence of trees on the spatial pattern of radiocesium on the forest floor

Kato et al. (2018a) reported that the ^{137}Cs inventory on the forest floor of the study site tended to increase as the distance from the nearest tree trunk increased in the early phase of the initial deposition (<1 y). This was possibly because the initial canopy interception decreased toward the canopy edge due to the lower canopy cover in the peripheral

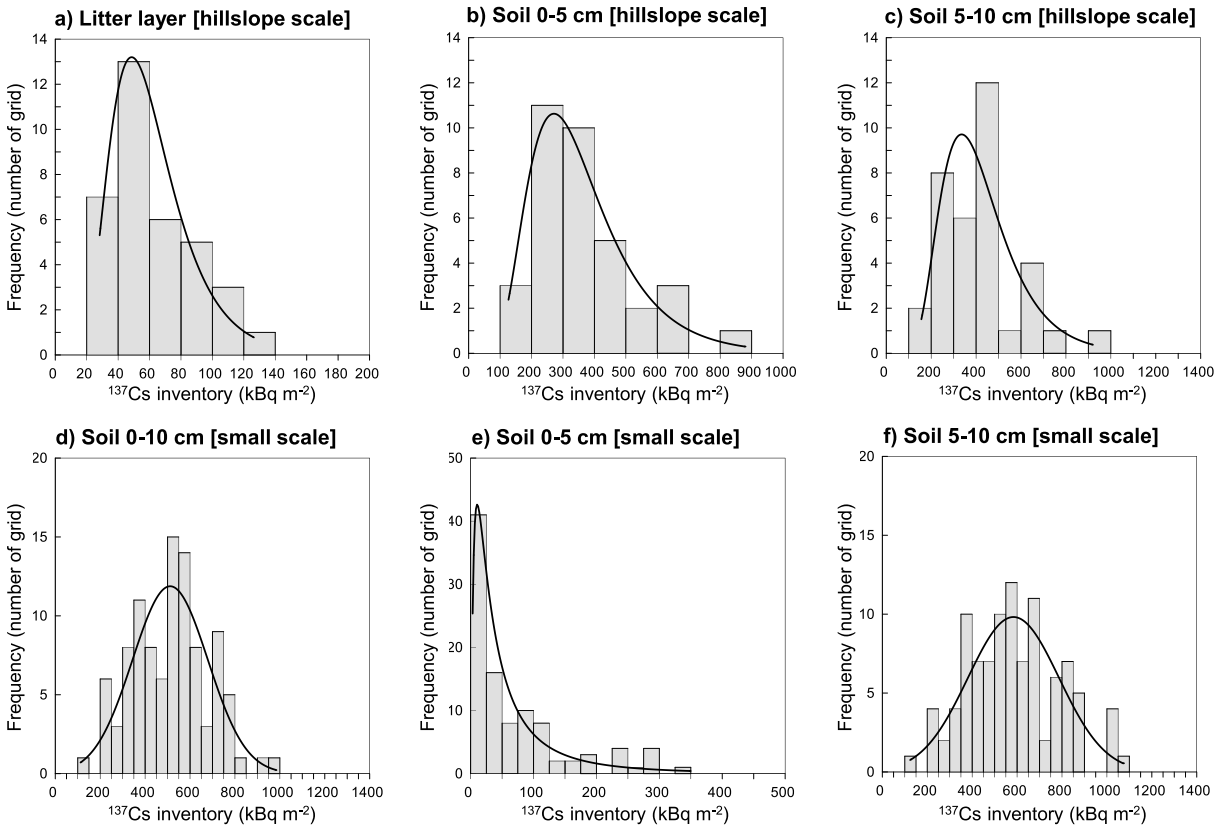

Fig. 4. Histogram of the ^{137}Cs inventory at the 49 sampling points within the hillslope-scale plot, and 100 points within the small-scale plot.

area of the forest. At both the hillslope and small scales, the ^{137}Cs inventory in the soil layer tended to increase with distance from the nearest tree trunk (Figure S-6b and S-7). Furthermore, there was no clear correlation between the distance from the nearest tree trunk and the ^{137}Cs inventory in the 5–10 cm soil layer for both the small scale and hillslope scale plots.

The study area was a planted forest that had not been thinned and had a very high density of standing trees (~2,400 trees/ha) (Coppin et al., 2016). As a result the canopy openings were very small (averaging 7.1%), even in the narrow measurement area. Therefore, there were no large gaps in the forest (open space without canopy), and ^{137}Cs was considered to have undergone canopy interception during deposition. The effects of canopy closure on the ^{137}Cs inventory on the forest floor were examined (Figure S-8); however, there was no significant correlation between canopy closure and the ^{137}Cs inventory in the deposited organic material or the mineral soil layer.

The canopy interception of rainwater and dissolved ions decreased toward the peripheral area of the canopy (Hansen et al., 1994; Hansen, 1996). As the distance from a tree trunk increases, the leaf area index (LAI) tends to decrease (Nanko et al., 2011). In this study, the ^{137}Cs inventory in soil tended to increase as the distance from a tree trunk increased. The results obtained in the study contradicted previous hydrological findings of the canopy regarding the amount of dissolved material entering the forest floor. The primary depositional input of ^{137}Cs to the surrounding land surface occurred within a month of the accident. Therefore, the higher ^{137}Cs inventory at the canopy edge represented the preservation of the distribution at the time of the initial deposition.

Although the experimental plot was located on a steep forested hillslope (<33°), the observed spatial pattern of ^{137}Cs on the forest floor was very similar to the initial depositional pattern of ^{137}Cs reported by Kato et al. (2018a). It is unlikely that ^{137}Cs, which is strongly adsorbed by clay minerals, would move laterally in the soil. Furthermore, the removal of ^{137}Cs due to decontamination accounted for less than 20% of the ^{137}Cs inventory on the forest floor, and forest decontamination was therefore unlikely to influence the spatial pattern of the ^{137}Cs inventory in the mineral soil layer.

3.3. *Optimization of the soil sampling strategy for determining a representative radiocesium inventory on a forest floor*

The CV was calculated for different sampling numbers (n) based on hillslope and small scale sampling results. The mean and SD of the ^{137}Cs inventories for the various samplings were calculated by a random sampling method (10,000 times for each sampling number) (Fig. 8). The SD of the mean ^{137}Cs inventory and the CV decreased with an increase in the total sampling area used to estimate the mean ^{137}Cs inventory within the target surface area.

When measurements are made using a field soil sampling method, the number of samples and method used should be determined according to the tolerance of uncertainty. By increasing the sampling area, the average radiocesium concentration obtained from the collected samples was closer to the actual value. The increase in sampling area is usually achieved by adding an arbitrary number of samples at and around the measurement site (Sutherland, 1998; Mabit et al., 2010). For the investigation of the radiocesium depth distribution in a forest soil, a device with a large sampling area such as a scraper plate of 0.15 × 0.30 m = 0.045 m^2 is often used to obtain a representative inventory of the target forest stand (Teramage et al., 2014b; Takahashi et al., 2015, 2018).

Khomutinin et al. (2004, 2020) found that the radioactivity concentration at a given point in a contaminated research area is defined by three factors: (1) the contamination trend, (2) spot points of contamination, and (3) random contamination. The contamination trend will indicate the amount of deposition from a global perspective, while spot points of contamination can indicate a regional increase or decrease in

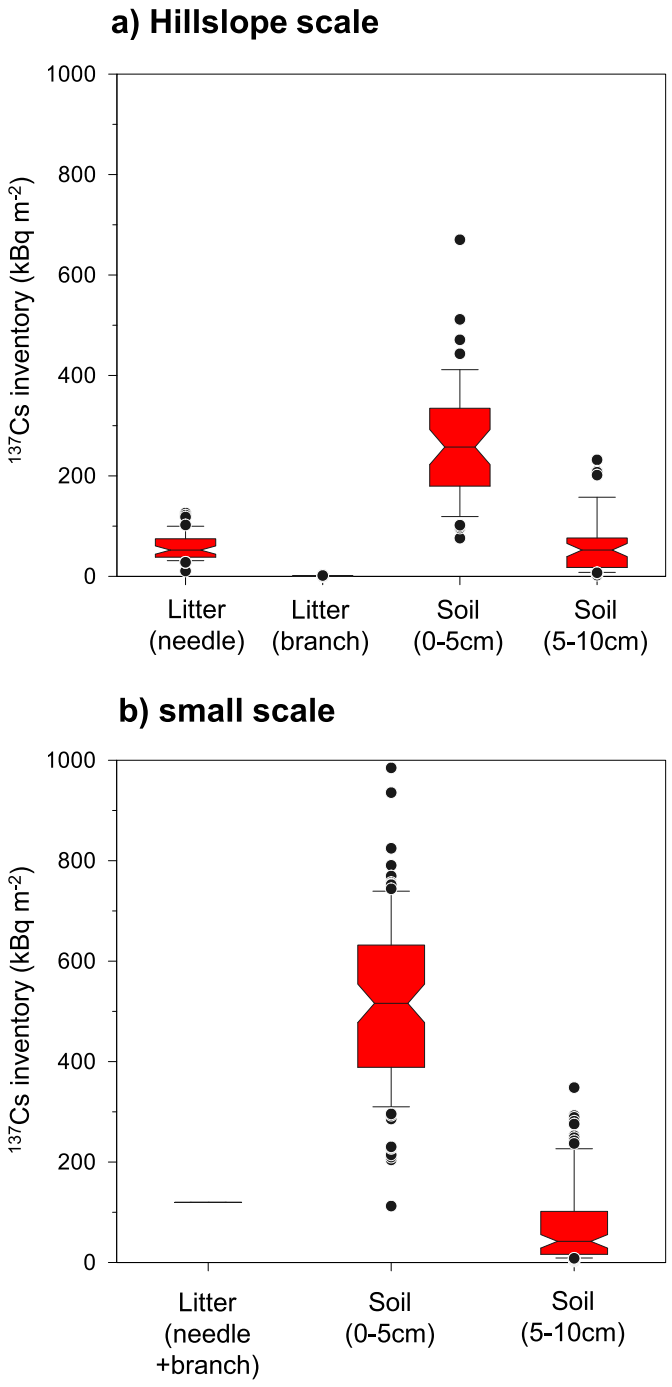

Fig. 5. Cesium-137 inventory in different layer components of forest floor. The percentage numbers in the diagram represent the ratio of the contained inventory in each layer to the total aerial inventory.

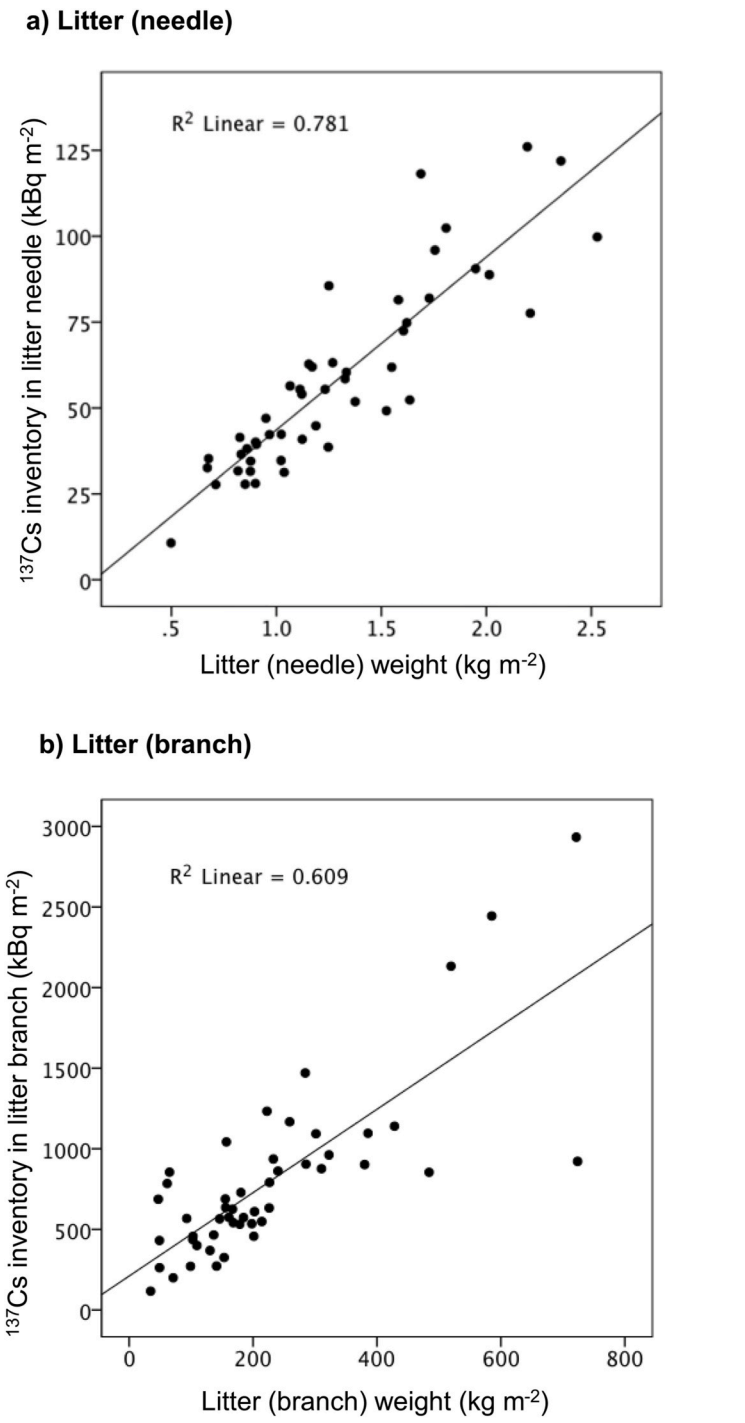

Fig. 6. Relationship between mass weight and ^{137}Cs inventory of the deposited organic material at the 49 sampling points within the hillslope scale plot.

concentration in relation to the contamination trend. Random contamination indicates the spatial unevenness of local concentrations, which may be influenced by sampling techniques and methods. The choice of sampling method can be an essential factor determining data values in the measurement of environmental radioactivity. In this study, a 60 m^2 area was sampled to obtain data that could be used to evaluate random contamination in the cedar forest. The sampling data obtained in this study were used to evaluate the relationship between the number of samples and the tolerance of the sampling results from the forest stand.

Soil samples were collected at five points per grid using a cylindrical soil core sampler with a sampling area of 0.00196 m^2. The tolerance of the measurements was assessed using data obtained from 100-point sampling (Figure S-9). The resulting CV values for five core samplings was 15.2% at soil depths of 0–10 cm. If the allowable error was a CV of 20%, it was found that a four-point sampling (total sampling area of 0.00785 m^2) was sufficient for the small scale (<1 m^2).

We compared the dataset from this study and from Khomutinin et al. (2004, 2020) using the S_{so} parameter (SD of n-points sampling [$S_{n,so}$]/SD of 1-point sampling [$S_{1,so}$]) and its evolution with increasing sampling area (Fig. 8). These comparisons revealed a clear decrease in the SD when the sampling area of the forest was increased. The scraper plate (0.045 m^2) corresponded to an area of 22.9 core samplers, resulting in a normalized SD ($S_{n,so}/S_{1,so}$) of 0.47. These results indicated

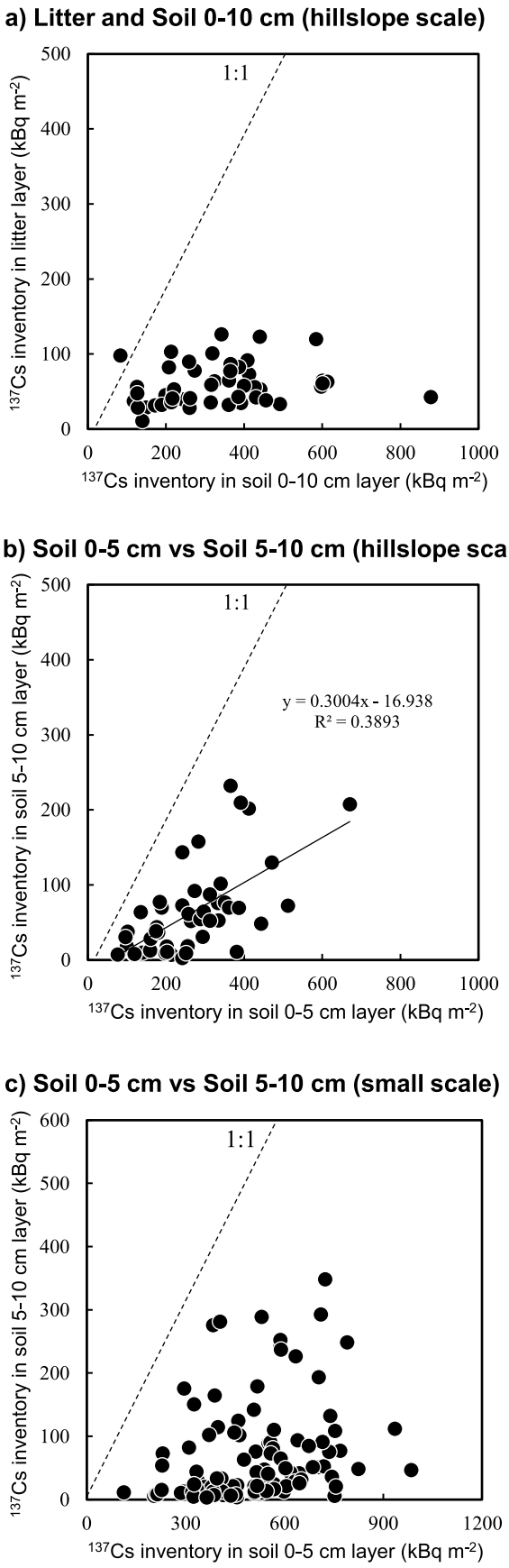

Fig. 7. Comparison of ^{137}Cs inventories in different layer components of the forest floor at the 49 sampling points within the hillslope scale plot and 100 points within small scale plot.

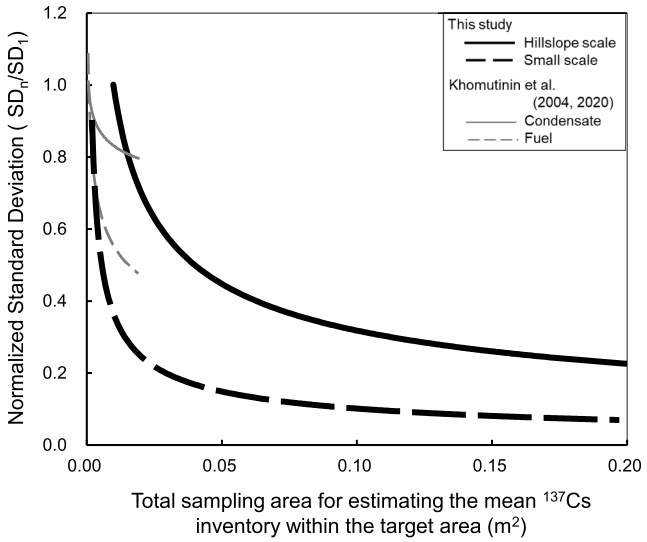

Fig. 8. Relationship between total sampling area and the normalized standard deviation for the mean ^{137}Cs inventory, for the hillslope and small scales, and comparison with those derived from the previous studies in Chernobyl accident affected area.

that increasing the total sampling area reduced the uncertainties in determining the mean ^{137}Cs inventory on the forest floor of the Japanese cedar stand. In comparison with previous studies, it was found that the grassland affected by condensate deposition from the Chernobyl accident exhibited a more distinct variation in its ^{137}Cs inventory than the forest floor affected by the Fukushima accident. To obtain the average ^{137}Cs inventory at the scale of interest with an error of less than 20%, it is necessary to take an area of 0.06 m^2 at the slope scale (60 m^2) and more than 0.008 m^2 at the small scale (1 m^2).

4. Conclusion

In this study, the spatial distribution of radiocesium on the forest floor of an artificial cedar forest was determined by litter and soil sampling. The factors responsible for the heterogeneity of ^{137}Cs were investigated in slope-scale (60 m^2) and small-scale (1 m^2) experimental plots established on the stand's hillslope. Litter–soil sampling was conducted by systematically dividing the plot area into grids. The target forest area had been decontaminated by removing deposited organic matter prior to this study. The litter layer accumulated between decontamination and sampling during the sampling campaign. Thus, the spatial distributions of ^{137}Cs deposition due to hydrological and litterfall pathways were evaluated separately.

This study showed that the ^{137}Cs inventories in the forest floor litter and soil layers were heterogeneously distributed and had a lognormal distribution at both hillslope and small scales. On average, about 70% of the ^{137}Cs in the forest floor was present in the 0–5-cm soil layer, about 15% was present in the litter, and the remainder was present in the 5–10-cm soil layer. At the hillslope scale, the ^{137}Cs inventories in the 0–5 and 5–10-cm soil layers were correlated, but there was no correlation between the soil and litter layers. This suggests that the litter ^{137}Cs input after decontamination did not represent the flux of ^{137}Cs into the soil layer, although the ^{137}Cs inventory increased in the 5–10-cm layer at sites with a high ^{137}Cs flux to the surface soil. On the other hand, no significant correlation was observed between the ^{137}Cs inventory of the 0–5-cm surface layer and the 5–10-cm subsoil layer at the small scale, suggesting that preferential and bypass flow may contribute to the vertical and lateral transport of radiocesium in the soil layer.

The ^{137}Cs inventory in the soil tended to increase toward the peripheral area of the tree canopy at both the hillslope and small scales. It

was likely that the spatial patterns of ^{137}Cs in the soil layer preserved the heterogeneous depositional input due to initial canopy interception during atmospheric fallout. However, there was no clear trend in the ^{137}Cs inventory in the deposited organic layer under a dense closed canopy cover.

Based on the spatial distribution of the ^{137}Cs inventory on the forest floor, the soil sampling method necessary to obtain a representative ^{137}Cs inventory of the forest floor at the hillslope or small scale was examined. To obtain the average ^{137}Cs inventory at the scale of interest with an error of less than 20%, it was necessary to take an area of 0.06 m^2 at the hillslope scale (60 m^2) and more than 0.008 m^2 at the small scale (1 m^2).

Radiocesium concentrations and inventories in the soil can be used as base data for concentration ratios and aggregate transfer factors, for example, which are transfer parameters for plants and animals in forest ecosystems. However, as the results of this study demonstrate, radiocesium on the forest floor is very variable in the horizontal and vertical directions. Depending on how the soil is sampled, significant uncertainties arise in estimates of transfer parameters. This study provides guidelines for obtaining representative data on the characteristics of radiocesium distribution on the forest floor and its determinants in cedar forests, which are common in the areas affected by the Fukushima Nuclear Power Plant accident. Developing sampling plans with consideration of the results of this study should improve the accuracy of research on the transfer mechanisms of radionuclides and dose assessment in forest environments.

Declaration of competing interest

The authors declare that they have no known competing financial interests or personal relationships that could have appeared to influence the work reported in this paper.

Acknowledgment

This work was conducted as a commissioned study from the Japanese Atomic Energy Agency, as a part of the Ministry of Education, Culture, Sports, Science and Technology-funded FY2011-2012, the Nuclear Regulation Authority of Japan-funded FY 2012–2014, and the Japanese Atomic Energy Agency-funded FY2015-2016. In addition, this work was partially supported by JSPS KAKENHI, Grant-in-Aid for Scientific Research (C) (#20K06140), Grant-in-Aid for Scientific Research on Innovative Areas (#2409, and Research in a proposed research area; #15H00969), and Grant-in-Aid for Young Scientists (B) (#16K16201) from the Japan Society for the Promotion of Science.

Appendix A. Supplementary data

Supplementary data to this article can be found online at https://doi.org/10.1016/j.jenvman.2022.115064.

The English in this document has been checked by at least two professional editors, both native speakers of English. For a certificate, please see: http://www.textcheck.com/certificate/Mu5cIz.

References

Atarashi-Andoh, M., Koarashi, J., Takeuchi, E., Tsuduki, K., Nishimura, S., Matsunaga, T., 2015. Catchment-scale distribution of radiocesium air dose rate in a mountainous deciduous forest and its relation to topography. J. Environ. Radioact. 147, 1–7. https://doi.org/10.1016/j.jenvrad.2015.05.004.

Bengough, A.G., 2012. Water dynamics of the root zone: rhizosphere biophysics and its control on soil hydrology. Vadose Zone J. 11 (2), 0111 vzj2011.

Bunzl, K., Schimmack, W., Kreutzer, K., 1989. Interception and retention of Chernobyl-derived ^{134}Cs, ^{137}Cs and ^{106}Ru in a spruce stand. Sci. Total Environ. 78, 77–87.

Butler, D., 2011. Radioactivity spreads in Japan. Nature 471, 555–556. https://doi.org/10.1038/471555a.

Chiang, P.N., Wang, M.K., Huang, P.M., Wang, J.J., 2011. Effects of low molecular weight organic acids on (137)Cs release from contaminated soils. Appl. Radiat. Isot. 69 (6), 844–851.

Conde Bueno, P., Martín Rubí, J.A., Jiménez Ballesta, R., 2008. Environmental evaluation of elemental cesium and strontium contents and their isotopic activity concentrations in different soils of La Mancha (Central Spain). Environ. Geol. 56, 327–334. https://doi.org/10.1007/s00254-007-1168-x.

Coppin, F., Hurtevent, P., Loffredo, N., Simonucci, C., Julien, A., Gonze, M.A., Nanba, K., Onda, Y., Thiry, Y., 2016. Radiocaesium partitioning in Japanese cedar forests following the "early" phase of Fukushima fallout redistribution. Sci. Rep. 6, 1–7. https://doi.org/10.1038/srep37618.

Cremers, A., Elsen, A., De Preter, P., Maes, A., 1988. Quantitative analysis of radiocaesium retention in soils. Nature 335, 247–249.

Dumat, C., Staunton, S., 1999. Reduced adsorption of caesium on clay minerals caused by various humic substances. J. Environ. Radioact. 46, 187–200.

Endo, I., Ohte, N., Iseda, K., Tanoi, K., Hirose, A., Kobayashi, N.I., Murakami, M., Tokuchi, N., Ohashi, M., 2015. Estimation of radioactive 137-cesium transportation by litterfall, stemflow and throughfall in the forests of Fukushima. J. Environ. Radioact. 149, 176–185. https://doi.org/10.1016/j.jenvrad.2015.07.027.

Fan, Q., Tanaka, M., Tanaka, K., Sakaguchi, A., Takahashi, Y., 2014. An EXAFS study on the effects of natural organic matter and the expandability of clay minerals on cesium adsorption and mobility. Geochem. Cosmochim. Acta 135, 49–65.

Fujii, K., Ikeda, S., Akama, A., Komatsu, M., Takahashi, M., Kaneko, S., 2014. Vertical migration of radiocesium and clay mineral composition in five forest soils contaminated by the Fukushima nuclear accident. Soil Sci. Plant Nutr. 60, 751–764. https://doi.org/10.1080/00380768.2014.926781.

Fukuyama, T., Onda, Y., Takenaka, C., Walling, D.E., 2008. Investigating erosion rates within a Japanese cypress plantation using Cs-137 and Pb-210ex measurements. J. Geophys. Res. Earth Surf. 113 https://doi.org/10.1029/2007JF000657.

Gonze, M.A., Mourlon, C., Calmon, P., Manach, E., Debayle, C., Baccou, J., 2016. Modelling the dynamics of ambient dose rates induced by radiocaesium in the Fukushima terrestrial environment. J. Environ. Radioact. 161, 22–34. https://doi.org/10.1016/j.jenvrad.2015.06.003.

Gonze, M.A., Mourlon, C., Calmon, P., Manach, E., Debayle, C., Gurriaran, R., Baccou, J., 2015. Assessment study of ambient dose rates dynamics in the Fukushima terrestrial region. 7th European Rev. Meet. Sev. Accid. Res. 24–26.

Hansen, K., 1996. In-canopy throughfall measurements of ion fluxes in Norway spruce. Atmos. Environ. 30, 4065–4076. https://doi.org/10.1016/1352-2310(95)00444-0.

Hansen, K., Draaijers, G.P.J., Ivens, W.P.M.F., Gundersen, P., van Leeuwen, N.F.M., 1994. Concentration variations in rain and canopy throughfall collected sequentially during individual rain events. Atmos. Environ. 28, 3195–3205. https://doi.org/10.1016/1352-2310(94)00176-L.

Hashimoto, S., Ugawa, S., Nanko, K., Shichi, K., 2012. The total amounts of radioactively contaminated materials in forests in Fukushima, Japan. Sci. Rep. 2, 1–5. https://doi.org/10.1038/srep00416.

Hisadome, K., Onda, Y., Loffredo, N., Kawamori, A., Kato, H., 2020. Spatial variation and radiocesium flux of litterfall in hardwood-pine mixed forest and cedar plantations based on long-term monitoring data. J. Radioanal. Nucl. Chem. 326, 1491–1504. https://doi.org/10.1007/s10967-020-07433-w.

IAEA, 2019. Guidelines on soil and vegetation sampling for radiological monitoring. Tech. Reports Ser. No. 486.

Imamura, N., Kobayashi, M., Kaneko, S., 2018. Forest edge effect in a radioactivity contaminated forest in Fukushima, Japan. J. For. Res. 23, 15–20. https://doi.org/10.1080/13416979.2017.1396417.

Imamura, N., Komatsu, M., Hashimoto, S., Fujii, K., Kato, H., Thiry, Y., Shaw, G., 2020. Vertical distributions of radiocesium in Japanese forest soils following the Fukushima Daiichi Nuclear Power Plant accident: a meta-analysis. J. Environ. Radioact. 225, 106422. https://doi.org/10.1016/j.jenvrad.2020.106422.

Itoh, Y., Imaya, A., Kobayashi, M., 2015. Initial radiocesium deposition on forest ecosystems surrounding the Tokyo metropolitan area due to the Fukushima Daiichi nuclear power plant accident. Hydrol. Res. Lett. 9, 1–7. https://doi.org/10.3178/hrl.9.1.

Kato, H., Onda, Y., 2018. Determining the initial Fukushima reactor accident-derived cesium-137 fallout in forested areas of municipalities in Fukushima Prefecture. J. For. Res. 23, 73–84. https://doi.org/10.1080/13416979.2018.1448566.

Kato, H., Onda, Y., 2014. Temporal changes in the transfer of accidently released 137Cs from tree crowns to the forest floor after the Fukushima Daiichi Nuclear Power Plant accident. Prog. Nucl. Sci. Technol. 4, 18–22. https://doi.org/10.15669/pnst.4.18.

Kato, H., Onda, Y., Gao, X., Sanada, Y., Saito, K., 2019a. Reconstruction of a Fukushima accident-derived radiocesium fallout map for environmental transfer studies. J. Environ. Radioact. 210, 105996. https://doi.org/10.1016/j.jenvrad.2019.105996.

Kato, H., Onda, Y., Gomi, T., 2012. Interception of the Fukushima reactor accident-derived 137Cs, 134Cs and 131I by coniferous forest canopies. Geophys. Res. Lett. 39, 1–6. https://doi.org/10.1029/2012GL052928.

Kato, H., Onda, Y., Hisadome, K., Loffredo, N., Kawamori, A., 2017. Temporal changes in radiocesium deposition in various forest stands following the Fukushima Dai-ichi Nuclear Power Plant accident. J. Environ. Radioact. 166, 449–457. https://doi.org/10.1016/j.jenvrad.2015.04.016.

Kato, H., Onda, Y., Wakahara, T., Kawamori, A., 2018a. Spatial pattern of atmospherically deposited radiocesium on the forest floor in the early phase of the Fukushima Daiichi Nuclear Power Plant accident. Sci. Total Environ. 615, 187–196. https://doi.org/10.1016/j.scitotenv.2017.09.212.

Kato, H., Onda, Y., Yamaguchi, T., 2018b. Temporal changes of the ambient dose rate in the forest environments of Fukushima Prefecture following the Fukushima reactor accident. J. Environ. Radioact. 193–194, 20–26. https://doi.org/10.1016/j.jenvrad.2018.08.009.

Kato, H., Onda, Y., Saidin, Z.H., Sakashita, W., Hisadome, K., Loffredo, N., 2019. Six-year monitoring study of radiocesium transfer in forest environments following the

Fukushima nuclear power plant accident. J. Environ. Radioact. 210, 105817. https://doi.org/10.1016/j.jenvrad.2018.09.015.
Khomutinin, Y.V., Kashparov, V.A., Zhebrovska, K.I., 2004. Sampling Optimisation when Radioecological Monitoring, 966-646-034-3. UIAR, p. 133, 2004.
Khomutinin, Y., Fesenko, S., Levchuk, S., Zhebrovska, K., Kashparov, V., 2020. Optimising sampling strategies for emergency response: soil sampling. J. Environ. Radioact. 222, 106344. https://doi.org/10.1016/j.jenvrad.2020.106344.
Kliashtorin, A.L., Tikhomirov, F.A., Shcheglov, A.I., 1994. Vertical radionuclide transfer by infiltration water in forest soils in the 30-km Chernobyl accident zone. Sci. Total Environ. 157, 285–288. https://doi.org/10.1016/0048-9697(94)90591-6.
Koarashi, J., Atarashi-Andoh, M., Matsunaga, T., Sato, T., Nagao, S., Nagai, H., 2012. Factors affecting vertical distribution of Fukushima accident-derived radiocesium in soil under different land-use conditions. Sci. Total Environ. 431, 392–401. https://doi.org/10.1016/j.scitotenv.2012.05.041.
Koarashi, J., Atarashi-Andoh, M., Takeuchi, E., Nishimura, S., 2014. Topographic heterogeneity effect on the accumulation of Fukushima-derived radiocesium on forest floor driven by biologically mediated processes. Sci. Rep. 4 https://doi.org/10.1038/srep06853.
Liang, W., Kosugi, K., Mizuyama, T., 2009. A three-dimensional model of the effect of stemflow on soil water dynamics around a tree on a hillslope. J. Hydrol. 366 (1–4), 62–75.
Liang, W., Kosugi, K., Mizuyama, T., 2011. Soil water dynamics around a tree on a hillslope with or without rainwater supplied by stemflow. Water Resour. Res. 47 (2), W02541.
Loffredo, N., Onda, Y., Hurtevent, P., Coppin, F., 2015. Equation to predict the 137Cs leaching dynamic from evergreen canopies after a radio-cesium deposit. J. Environ. Radioact. 147, 100–107. https://doi.org/10.1016/j.jenvrad.2015.05.018.
Loffredo, N., Onda, Y., Kawamori, A., Kato, H., 2014. Modeling of leachable 137Cs in throughfall and stemflow for Japanese forest canopies after Fukushima Daiichi Nuclear Power Plant accident. Sci. Total Environ. 493, 701–707. https://doi.org/10.1016/j.scitotenv.2014.06.059.
Luo, Z., Niu, K., Xie, B., Zhang, L., Chen, X., Berndtsson, R., Du, J., Ao, J., Yang, L., Zhu, S., 2019. Influence of root distribution on preferential flow in deciduous and coniferous forest soils. Forests 10, 986. https://doi.org/10.3390/f10110986.
Mabit, L., Martin, P., Jankong, P., Toloza, A., Padilla-Alvarez, R., Zupanc, V., 2010. Establishment of control site baseline data for erosion studies using radionuclides: a case study in East Slovenia. J. Environ. Radioact. 101, 854–863. https://doi.org/10.1016/j.jenvrad.2010.05.008.
Malins, A., Kurikami, H., Nakama, S., Saito, T., Okumura, M., Machida, M., Kitamura, A., 2016. Evaluation of ambient dose equivalent rates influenced by vertical and horizontal distribution of radioactive cesium in soil in Fukushima Prefecture. J. Environ. Radioact. 151, 38–49. https://doi.org/10.1016/j.jenvrad.2015.09.014.
Martínez Cortizas, A., García-Rodeja Gayoso, E., Nóvoa Munõz, J.C., Pontevedra Pombal, X., Buurman, P., Terribile, F., 2003. Distribution of some selected major and trace elements in four Italian soils developed from the deposits of the Gauro and Vico volcanoes. Geoderma 117, 215–224.
Melin, J., Wallberg, L., Suomela, J., 1994. Distribution and retention of cesium and strontium in Swedish boreal forest ecosystems. Sci. Total Environ. 157, 93–105. https://doi.org/10.1016/0048-9697(94)90568-1.
Nanko, K., Onda, Y., Ito, A., Moriwaki, H., 2011. Spatial variability of throughfall under a single tree: experimental study of rainfall amount, raindrops, and kinetic energy. Agric. For. Meteorol. 151, 1173–1182. https://doi.org/10.1016/j.agrformet.2011.04.006.
Niizato, T., Abe, H., Mitachi, K., Sasaki, Y., Ishii, Y., Watanabe, T., 2016. Input and output budgets of radiocesium concerning the forest floor in the mountain forest of Fukushima released from the TEPCO's Fukushima Dai-ichi nuclear power plant accident. J. Environ. Radioact. 161, 11–21. https://doi.org/10.1016/j.jenvrad.2016.04.017.
Nishikiori, T., Watanabe, M., Koshikawa, M.K., Takamatsu, T., Ishii, Y., Ito, S., Takenaka, A., Watanabe, K., Hayashi, S., 2015. Uptake and translocation of radiocesium in cedar leaves following the Fukushima nuclear accident. Sci. Total Environ. 502, 611–616. https://doi.org/10.1016/j.scitotenv.2014.09.063.
Palumbo, B., Angelone, M., Bellanca, A., Dazzi, C., Hauser, S., Neri, R., Wilson, J., 2000. Influence of inheritance and pedogenesis on heavy metal distribution in soils of Sicily. Italy. Geoderma 95, 247–266.
Ronneau, C., Cara, J., Apers, D., 1987. The deposition of radionuclides from Chernobyl to a forest in Belgium. Atmos. Environ. 21, 1467–1468. https://doi.org/10.1016/0004-6981(67)90094-7.
Schimmack, W., Förster, H., Bunzl, K., Kreutzer, K., 1993. Deposition of radiocesium to the soil by stemflow, throughfall and leaf-fall from beech trees. Radiat. Environ. Biophys. 32, 137–150. https://doi.org/10.1007/BF01212800.
Sombré, L., Vanhouche, M., de Brouwer, S., Ronneau, C., Lambotte, J.M., Myttenaere, C., 1994. Long-term radiocesium behaviour in spruce and oak forests. Sci. Total Environ. 157, 59–71. https://doi.org/10.1016/0048-9697(94)90565-7.
Sutherland, R.A., 1998. The potential for reference site resampling in estimating sediment redistribution and assessing landscape stability by the caesium-137 method. Hydrol. Process. 12, 995–1007. https://doi.org/10.1002/(SICI)1099-1085(19980615)12:7<995::AID-HYP634>3.0.CO;2-F.
Takada, M., Yamada, T., Takahara, T., Okuda, T., 2016. Spatial variation in the 137Cs inventory in soils in a mixed deciduous forest in Fukushima, Japan. J. Environ. Radioact. 161, 35–41. https://doi.org/10.1016/j.jenvrad.2016.04.033.
Takahashi, J., Tamura, K., Suda, T., Matsumura, R., Onda, Y., 2015. Vertical distribution and temporal changes of 137Cs in soil profiles under various land uses after the Fukushima Dai-ichi Nuclear Power Plant accident. J. Environ. Radioact. 139, 351–361. https://doi.org/10.1016/j.jenvrad.2014.07.004.
Takahashi, J., Onda, Y., Hihara, D., Tamura, K., 2018. Six-year monitoring of the vertical distribution of radiocesium in three forest soils after the Fukushima Dai-ichi Nuclear Power Plant accident. J. Environ. Radioact. 192, 172–180. https://doi.org/10.1016/j.jenvrad.2018.06.015.
Tatsuno, T., Hamamoto, S., Nihei, N., Nishimura, T., 2020. Effects of the dissolved organic matter on Cs transport in the weathered granite soil. J. Environ. Manag. 254, 109785.
Teramage, M.T., Onda, Y., Kato, H., Gomi, T., 2014a. The role of litterfall in transferring Fukushima-derived radiocesium to a coniferous forest floor. Sci. Total Environ. 490, 435–439. https://doi.org/10.1016/j.scitotenv.2014.05.034.
Teramage, M.T., Onda, Y., Patin, J., Kato, H., Gomi, T., Nam, S., 2014b. Vertical distribution of radiocesium in coniferous forest soil after the Fukushima nuclear power plant accident. J. Environ. Radioact. 137, 37–45. https://doi.org/10.1016/j.jenvrad.2014.06.017.
Tracy, S.R., Black, C.R., Roberts, J.A., Mooney, S.J., 2013. Exploring the interacting effect of soil texture and bulk density on root system development in tomato (Solanum lycopersicum L.). Environ. Exp. Bot. 91, 38–47.
Wendling, L.A., Harsh, J.B., Ward, T.E., Palmer, C.D., Hamilton, M.A., Boyle, J.S., Flury, M., 2005. Cesium desorption from illite as affected by exudates from rhizosphere bacteria. Environ. Sci. Technol. 39 (12), 4505–4512.
Zhang, Y.H., Niu, J.Z., Yu, X.X., Zhu, W.L., Du, X.Q., 2015. Effects of fine root length density and root biomass on soil preferential flow in forest ecosystems. For. Syst. 24 (1), e012.